Supplement of Nat. Hazards Earth Syst. Sci., 24, 331–354, 2024
https://doi.org/10.5194/nhess-24-331-2024-supplement

Natural Hazards and Earth System Sciences
Open Access

Supplement of

High-resolution projections of ambient heat for major European cities using different heat metrics

Clemens Schwingshackl et al.

Correspondence to: Clemens Schwingshackl (c.schwingshackl@lmu.de)

Supplementary Tables

Table S1: Overview of the 36 cities, their coordinates, elevation of the city centre, and whether a city is located close to the sea.

City	Latitude / °	Longitude / °	Elevation / m	Located close to sea?
Amsterdam	52.367	4.900	-2	yes
Athens	37.984	23.728	153	yes
Barcelona	41.383	2.183	12	yes
Belgrade	44.817	20.467	116	no
Berlin	52.517	13.383	34	no
Brussels	50.847	4.353	76	no
Bucharest	44.433	26.104	70	no
Budapest	47.493	19.051	102	no
Copenhagen	55.676	12.568	5	yes
Dublin	53.350	-6.267	8	yes
Hamburg	53.565	10.001	6	no
Helsinki	60.171	24.938	25	yes
Istanbul	41.014	28.955	40	yes
Kazan	55.790	49.135	116	no
Kharkiv	50.004	36.231	152	no
Kyiv	50.450	30.523	168	no
Lisbon	38.725	-9.150	15	yes
London	51.507	-0.128	14	no
Madrid	40.383	-3.717	667	no
Milan	45.467	9.183	152	no
Minsk	53.900	27.567	198	no
Moscow	55.750	37.617	124	no
Munich	48.133	11.567	520	no
Nizhny Novgorod	56.327	44.008	78	no
Oslo	59.914	10.752	12	yes
Paris	48.857	2.351	34	no
Prague	50.083	14.417	244	no
Riga	56.949	24.106	8	yes
Rome	41.900	12.500	14	no
Saint Petersburg	59.950	30.300	13	yes
Sofia	42.700	23.330	580	no
Stockholm	59.329	18.069	15	yes
Vienna	48.200	16.367	170	no
Vilnius	54.683	25.283	124	no
Warsaw	52.233	21.017	93	no
Zagreb	45.817	15.983	130	no

Table S2: Overview of the EURO-CORDEX regional climate models (RCMs) used in this study and the respective driving general circulation models (GCM). All simulations are performed using the EUR-11 resolution.

GCM	RCM	Ensemble member
CCCma-CanESM2	CLMcom-CCLM4-8-17	r1i1p1
CCCma-CanESM2	GERICS-REMO2015	r1i1p1
CNRM-CERFACS-CNRM-CM5	CLMcom-CCLM4-8-17	r1i1p1
CNRM-CERFACS-CNRM-CM5	CNRM-ALADIN53	r1i1p1
CNRM-CERFACS-CNRM-CM5	CNRM-ALADIN63	r1i1p1
CNRM-CERFACS-CNRM-CM5	DMI-HIRHAM5	r1i1p1
CNRM-CERFACS-CNRM-CM5	GERICS-REMO2015	r1i1p1
CNRM-CERFACS-CNRM-CM5	IPSL-WRF381P	r1i1p1
CNRM-CERFACS-CNRM-CM5	KNMI-RACMO22E	r1i1p1
CNRM-CERFACS-CNRM-CM5	SMHI-RCA4	r1i1p1
CNRM-CERFACS-CNRM-CM5	CLMcom-ETH-COSMO-crCLIM-v1-1	r1i1p1
CNRM-CERFACS-CNRM-CM5	ICTP-RegCM4-6	r1i1p1
CNRM-CERFACS-CNRM-CM5	MOHC-HadREM3-GA7-05	r1i1p1
ICHEC-EC-EARTH	CLMcom-CCLM4-8-17	r12i1p1
ICHEC-EC-EARTH	CLMcom-ETH-COSMO-crCLIM-v1-1	r12i1p1
ICHEC-EC-EARTH	CLMcom-ETH-COSMO-crCLIM-v1-1	r1i1p1
ICHEC-EC-EARTH	CLMcom-ETH-COSMO-crCLIM-v1-1	r3i1p1
ICHEC-EC-EARTH	DMI-HIRHAM5	r12i1p1
ICHEC-EC-EARTH	DMI-HIRHAM5	r1i1p1
ICHEC-EC-EARTH	DMI-HIRHAM5	r3i1p1
ICHEC-EC-EARTH	GERICS-REMO2015	r12i1p1
ICHEC-EC-EARTH	ICTP-RegCM4-6	r12i1p1
ICHEC-EC-EARTH	IPSL-WRF381P	r12i1p1
ICHEC-EC-EARTH	KNMI-RACMO22E	r12i1p1
ICHEC-EC-EARTH	KNMI-RACMO22E	r1i1p1
ICHEC-EC-EARTH	KNMI-RACMO22E	r3i1p1
ICHEC-EC-EARTH	MOHC-HadREM3-GA7-05	r12i1p1
ICHEC-EC-EARTH	SMHI-RCA4	r12i1p1
ICHEC-EC-EARTH	SMHI-RCA4	r1i1p1
ICHEC-EC-EARTH	SMHI-RCA4	r3i1p1
IPSL-IPSL-CM5A-MR	DMI-HIRHAM5	r1i1p1
IPSL-IPSL-CM5A-MR	GERICS-REMO2015	r1i1p1
IPSL-IPSL-CM5A-MR	IPSL-WRF381P	r1i1p1
IPSL-IPSL-CM5A-MR	KNMI-RACMO22E	r1i1p1
IPSL-IPSL-CM5A-MR	SMHI-RCA4	r1i1p1
MIROC-MIROC5	CLMcom-CCLM4-8-17	r1i1p1
MIROC-MIROC5	GERICS-REMO2015	r1i1p1
MOHC-HadGEM2-ES	CLMcom-CCLM4-8-17	r1i1p1
MOHC-HadGEM2-ES	CLMcom-ETH-COSMO-crCLIM-v1-1	r1i1p1
MOHC-HadGEM2-ES	CNRM-ALADIN63	r1i1p1
MOHC-HadGEM2-ES	DMI-HIRHAM5	r1i1p1
MOHC-HadGEM2-ES	GERICS-REMO2015	r1i1p1
MOHC-HadGEM2-ES	ICTP-RegCM4-6	r1i1p1
MOHC-HadGEM2-ES	IPSL-WRF381P	r1i1p1

GCM	RCM	Ensemble member
MOHC-HadGEM2-ES	KNMI-RACMO22E	r1i1p1
MOHC-HadGEM2-ES	MOHC-HadREM3-GA7-05	r1i1p1
MOHC-HadGEM2-ES	SMHI-RCA4	r1i1p1
MPI-M-MPI-ESM-LR	CLMcom-CCLM4-8-17	r1i1p1
MPI-M-MPI-ESM-LR	CLMcom-ETH-COSMO-crCLIM-v1-1	r1i1p1
MPI-M-MPI-ESM-LR	CLMcom-ETH-COSMO-crCLIM-v1-1	r2i1p1
MPI-M-MPI-ESM-LR	CLMcom-ETH-COSMO-crCLIM-v1-1	r3i1p1
MPI-M-MPI-ESM-LR	CNRM-ALADIN63	r1i1p1
MPI-M-MPI-ESM-LR	DMI-HIRHAM5	r1i1p1
MPI-M-MPI-ESM-LR	GERICS-REMO2015	r3i1p1
MPI-M-MPI-ESM-LR	ICTP-RegCM4-6	r1i1p1
MPI-M-MPI-ESM-LR	KNMI-RACMO22E	r1i1p1
MPI-M-MPI-ESM-LR	MOHC-HadREM3-GA7-05	r1i1p1
MPI-M-MPI-ESM-LR	MPI-CSC-REMO2009	r1i1p1
MPI-M-MPI-ESM-LR	MPI-CSC-REMO2009	r2i1p1
MPI-M-MPI-ESM-LR	SMHI-RCA4	r1i1p1
MPI-M-MPI-ESM-LR	SMHI-RCA4	r2i1p1
MPI-M-MPI-ESM-LR	SMHI-RCA4	r3i1p1
MPI-M-MPI-ESM-LR	IPSL-WRF381P	r1i1p1
NCC-NorESM1-M	CLMcom-ETH-COSMO-crCLIM-v1-1	r1i1p1
NCC-NorESM1-M	CNRM-ALADIN63	r1i1p1
NCC-NorESM1-M	DMI-HIRHAM5	r1i1p1
NCC-NorESM1-M	GERICS-REMO2015	r1i1p1
NCC-NorESM1-M	IPSL-WRF381P	r1i1p1
NCC-NorESM1-M	KNMI-RACMO22E	r1i1p1
NCC-NorESM1-M	MOHC-HadREM3-GA7-05	r1i1p1
NCC-NorESM1-M	SMHI-RCA4	r1i1p1
NCC-NorESM1-M	ICTP-RegCM4-6	r1i1p1

Table S3: Overview of the CMIP5 models used in this study. Models are only considered if they reach 3 °C European warming (20-year ESAT average relative to 1981-2010) before 2100 in RCP8.5. Models used for constructing the EURO-CORDEX GCM ensemble are marked with an asterisk (*). Ensemble members indicated in parentheses are only used for the EURO-CORDEX GCM ensemble. The member r3i1p1 for EC-EARTH, which is used to drive several EURO-CORDEX RCMs, is not available from the ESGF servers.

Model	Ensemble member
ACCESS1-0	r1p1f1
ACCESS1-3	r1p1f1
bcc-csm1-1	r1p1f1
bcc-csm1-1-m	r1p1f1
BNU-ESM	r1p1f1
CanESM2*	r1p1f1
CESM1-CAM5	r1p1f1
CNRM-CM5*	r1p1f1
CSIRO-Mk3-6-0	r1p1f1
EC-EARTH*	r1i1p1 (r12i1p1)
GFDL-CM3	r1p1f1
GFDL-ESM2G	r1p1f1
GFDL-ESM2M	r1p1f1
HadGEM2-AO	r1p1f1
HadGEM2-CC	r1p1f1
HadGEM2-ES*	r1p1f1
IPSL-CM5A-LR	r1p1f1
IPSL-CM5A-MR*	r1p1f1
IPSL-CM5B-LR	r1p1f1
MIROC5*	r1p1f1
MPI-ESM-LR*	r1p1f1 (r2p1f1, r3p1f1)
MRI-CGCM3	r1p1f1
MRI-ESM1	r1p1f1
NorESM1-M*	r1p1f1

Table S4: Overview of the CMIP6 models used in this study.

Model	Ensemble member
ACCESS-CM2	r1i1p1f1
ACCESS-ESM1-5	r1i1p1f1
CNRM-CM6-1	r1i1p1f2
CNRM-CM6-1-HR	r1i1p1f2
CNRM-ESM2-1	r1i1p1f2
CanESM5	r1i1p1f1
EC-Earth3	r1i1p1f1
EC-Earth3-Veg	r1i1p1f1
FGOALS-g3	r1i1p1f1
GFDL-CM4	r1i1p1f1
GFDL-ESM4	r1i1p1f1
HadGEM3-GC31-LL	r1i1p1f3
HadGEM3-GC31-MM	r1i1p1f3
INM-CM4-8	r1i1p1f1
INM-CM5-0	r1i1p1f1
KACE-1-0-G	r1i1p1f1
KIOST-ESM	r1i1p1f1
MIROC-ES2L	r1i1p1f2
MPI-ESM1-2-HR	r1i1p1f1
MPI-ESM1-2-LR	r1i1p1f1
MRI-ESM2-0	r1i1p1f1
NorESM2-LM	r1i1p1f1
NorESM2-MM	r1i1p1f1
UKESM1-0-LL	r1i1p1f2

Supplementary Figures

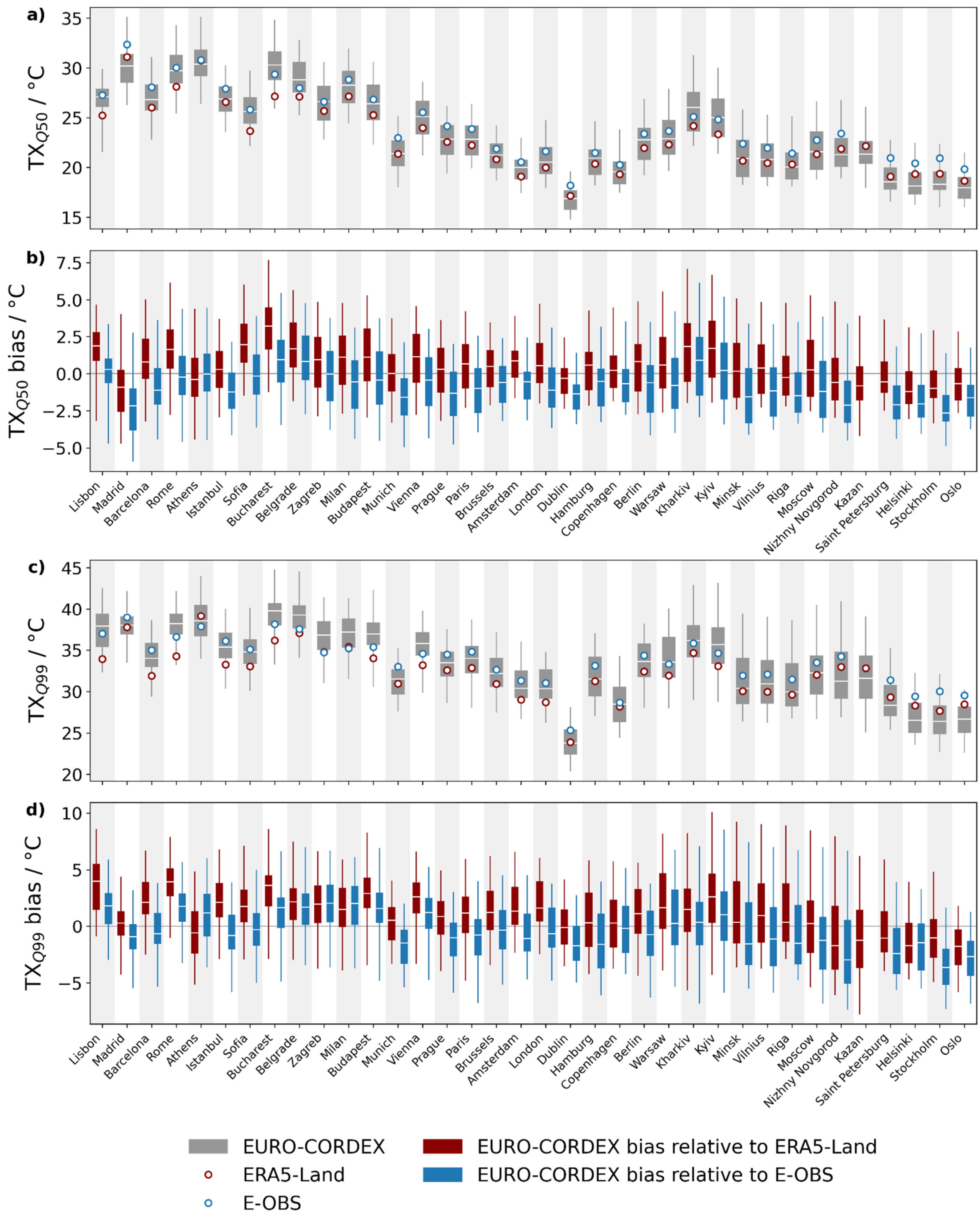

Figure S1: Comparison of EURO-CORDEX with ERA5-Land and E-OBS for daily maximum near-surface air temperature (TX) in summer (June, July, August) during 1981-2010. Panels a) and b) show the comparison for the TX median; panels c) and d) for the 99th quantile of TX. Panels a) and c) show the distribution of EURO-CORDEX models (grey box plots) versus ERA5-Land (red circles) and E-OBS (blue circles). Panels b) and d) show the EURO-CORDEX bias against ERA5-Land (red box plots) and E-OBS (blue box plots). Lines in the box plots indicate the median, boxes the interquartile range, and whiskers the minimum-to-maximum range.

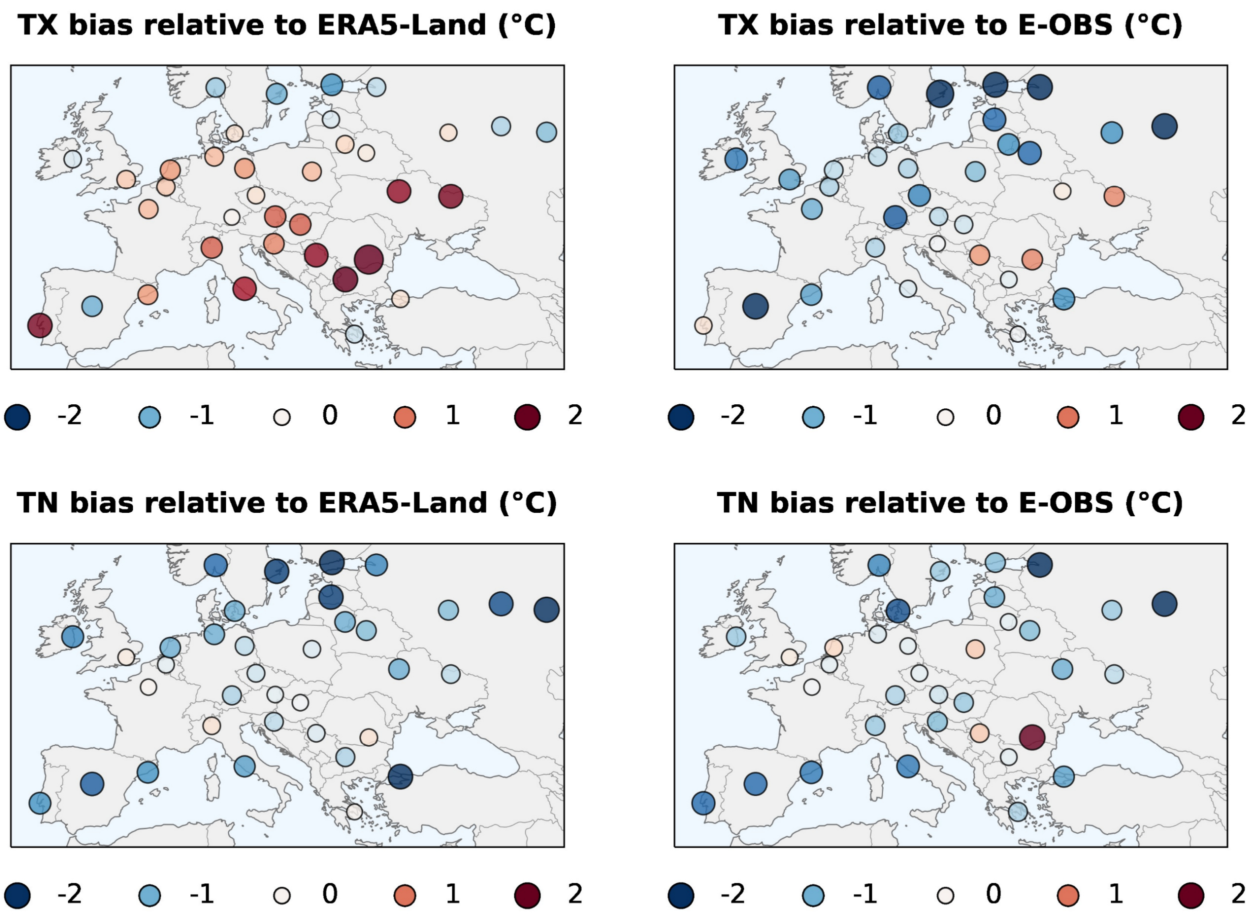

Figure S2: Maps of the multi-model median EURO-CORDEX bias relative to ERA5-Land and E-OBS for the median of daily maximum near-surface air temperature (TX) and the median of daily minimum near-surface air temperature (TN) in summer (June, July, August) during 1981-2010. For TX, the values correspond to the median values shown in Figure S1b.

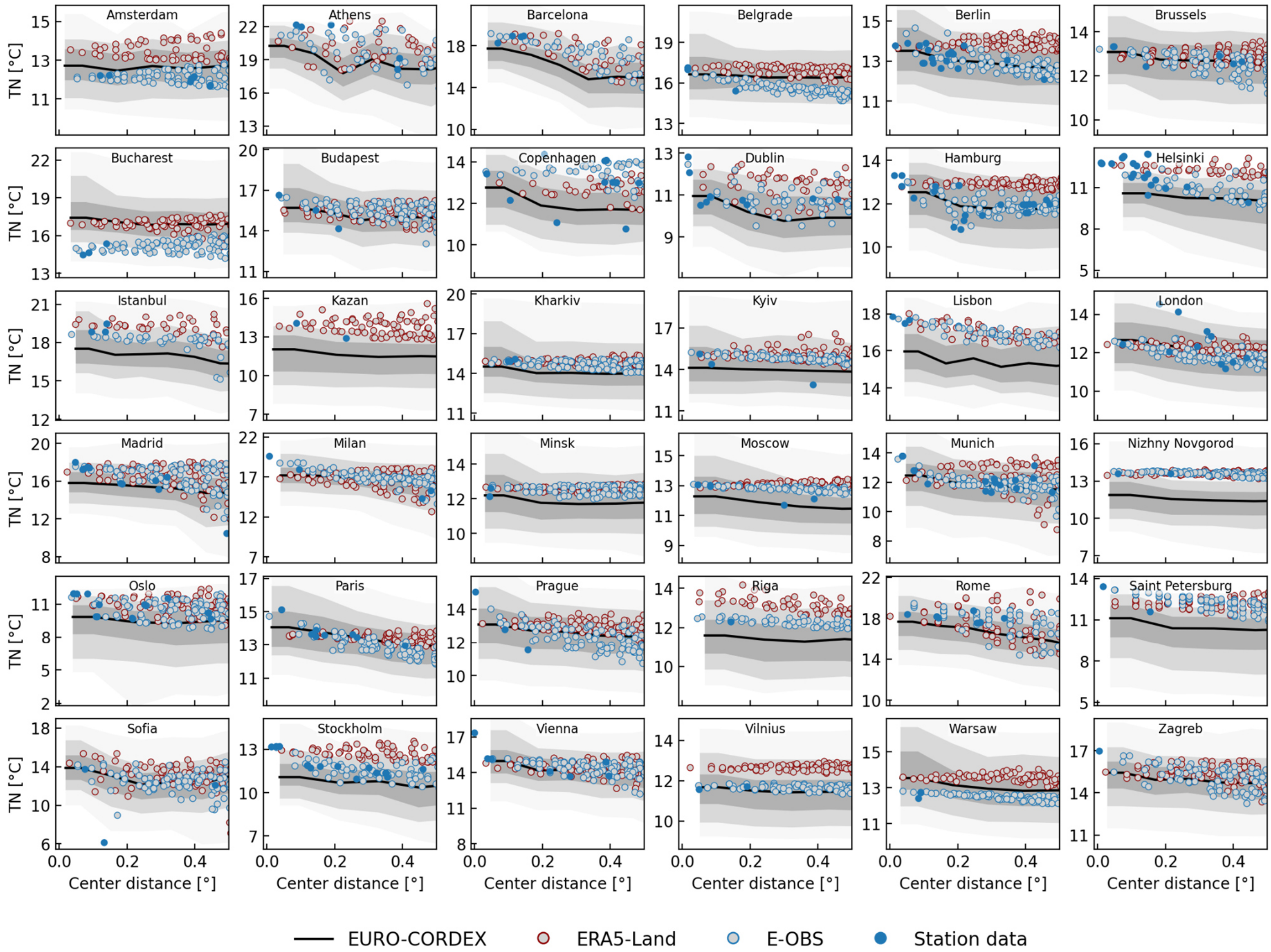

Figure S3: As in Figure 3 but for daily minimum near-surface air temperature (TN).

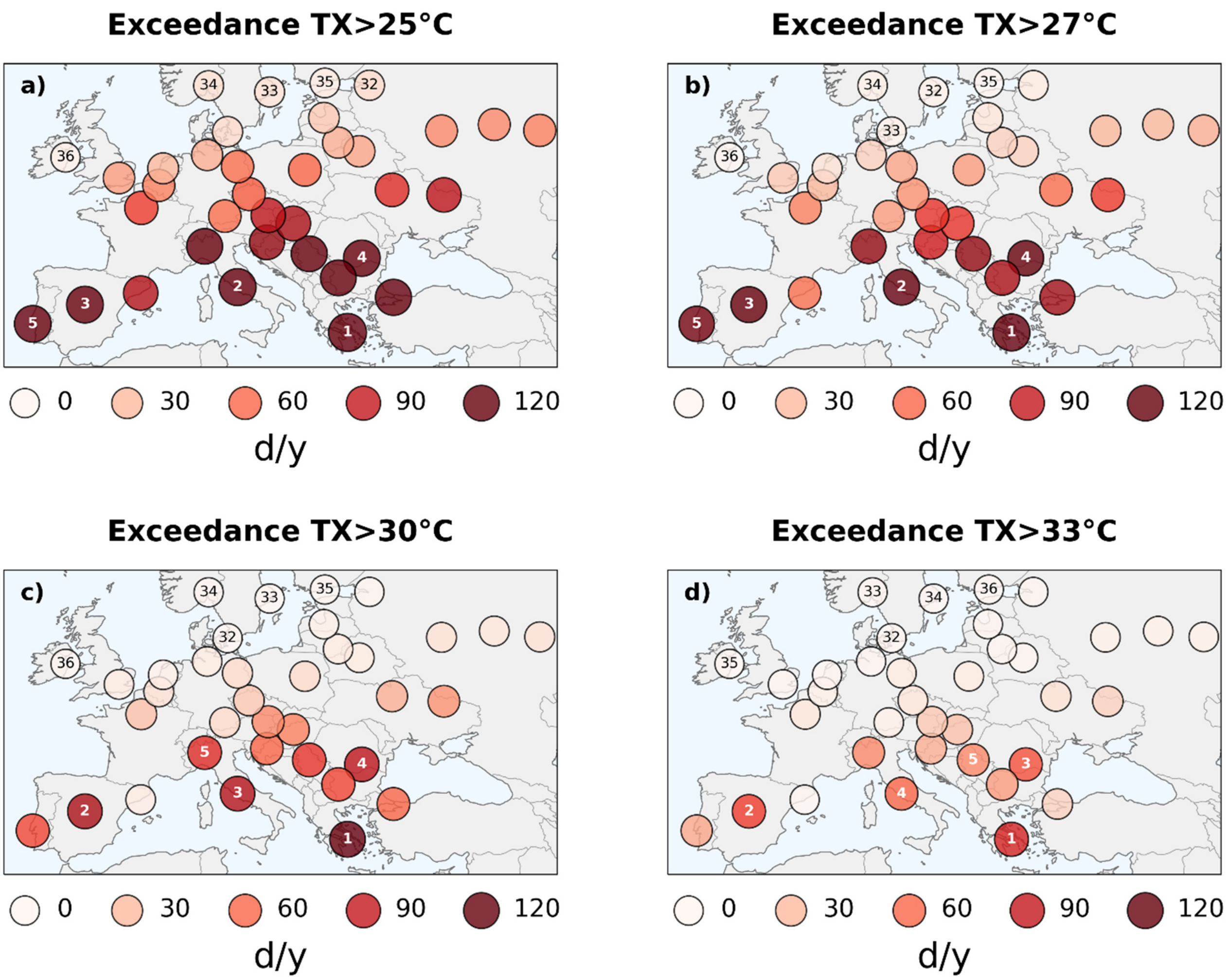

Figure S4: As in Figure 4 b) but for exceedances above a) 25 °C, b) 27 °C, c) 30 °C, and d) 33 °C.

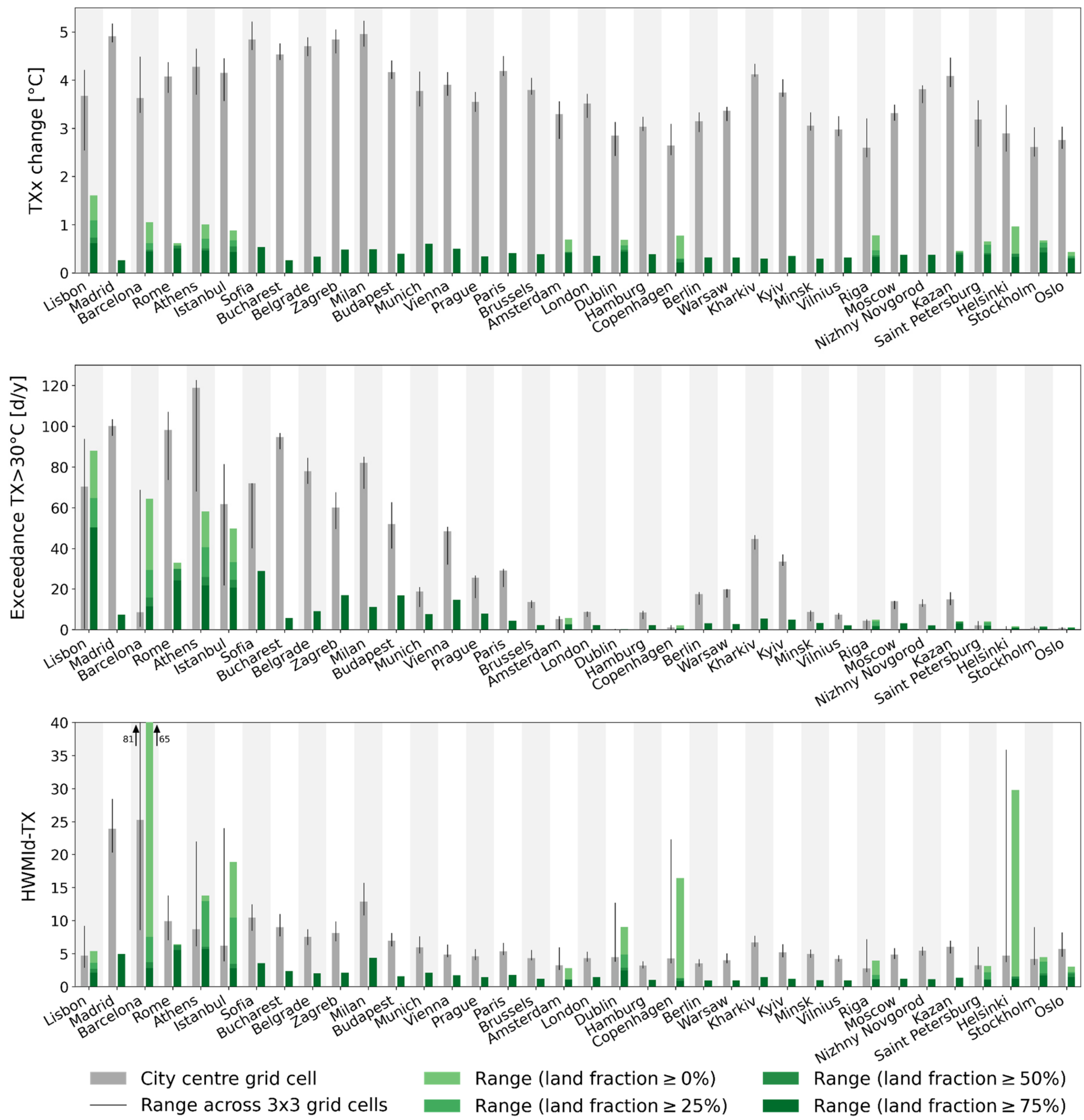

Figure S5: Comparison of ambient heat projections by the EURO-CORDEX ensemble for the grid cell closest to the centre of each city (grey bars; multi-model median) and variability in ambient heat projections within a box of 3x3 grid cells around the city centres (black whiskers and green bars) for a) change in yearly maximum near-surface air temperature (TXx) between 1981-2010 and 3 °C European warming, b) TX exceedances above 30 °C at 3 °C European warming, and c) Heat Wave Magnitude Index daily based on TX (HWMId-TX) at 3 °C European warming. Black whiskers denote the multi-model median of the minimum-to-maximum range across the 3x3 grid cells. Green bars also show the minimum-to-maximum range across grid cells, with the shading intensity indicating that only grid cells with varying degrees of minimum land fraction are considered (light green: all grid cells are considered; increasing shading intensity: only grid cells with at least 25%, 50%, and 75% land fraction are considered).

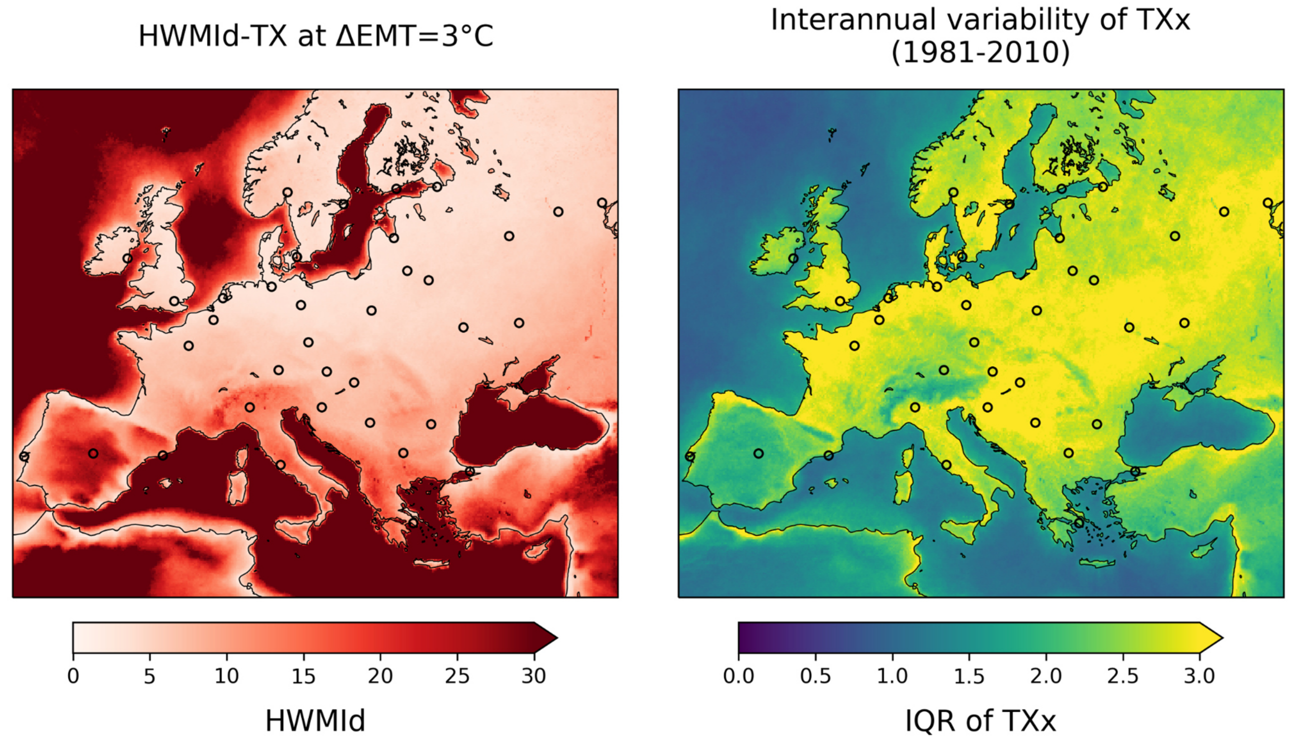

Figure S6: Heat Wave Magnitude Index daily based on daily maximum near-surface air temperature (HWMId-TX) at 3°C European warming and interannual variability (interquartile range) of yearly maximum near-surface air temperature (TXx) in the reference period 1981-2010. Both maps show the multi-model median of the EURO-CORDEX ensemble. Small black circles indicate the location of the 36 cities analysed in this study.

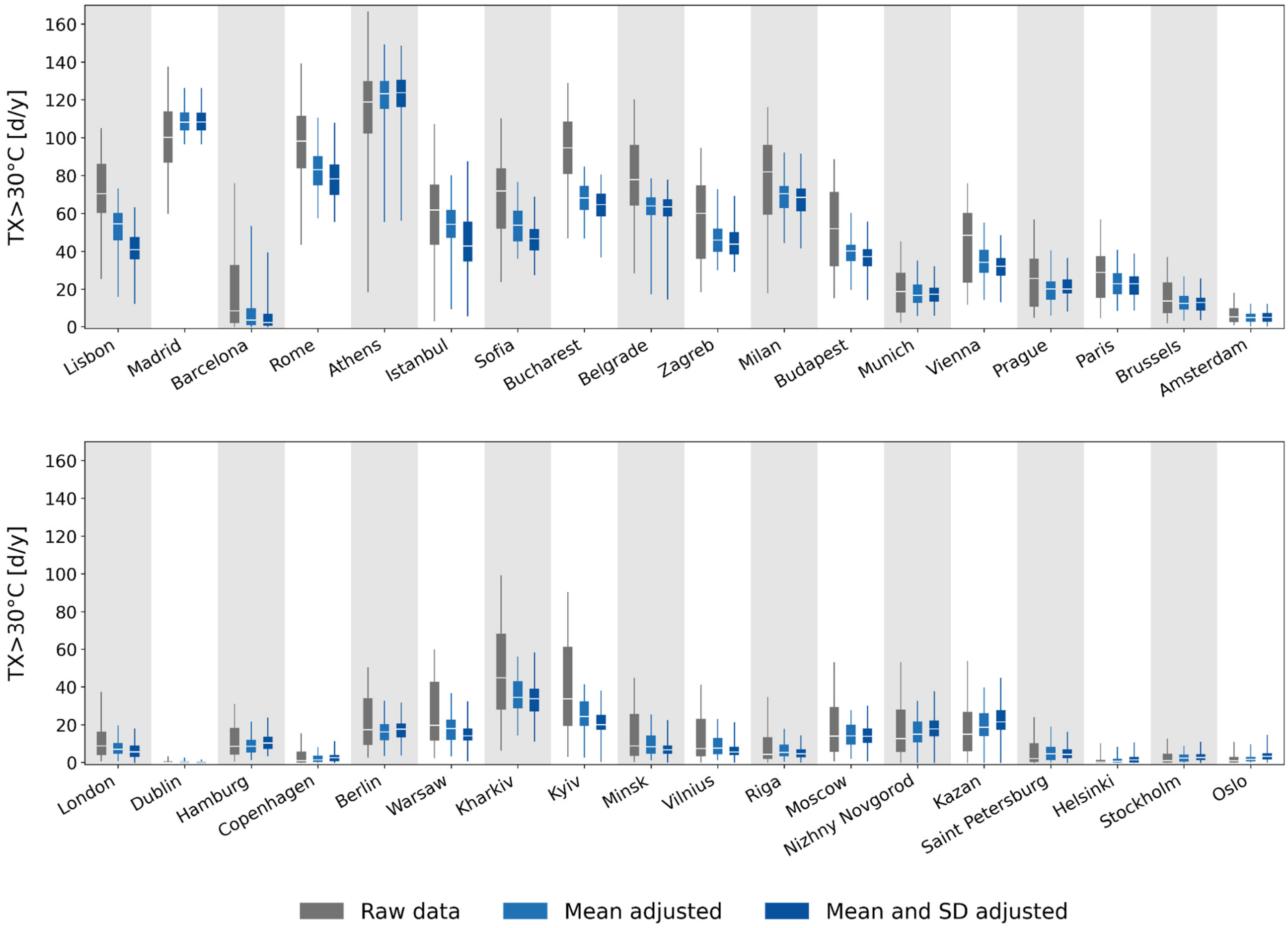

Figure S7: Sensitivity analysis for TX exceedances above 30 °C at 3 °C European warming. Grey box plots show estimates based on the original EURO-CORDEX data, light blue box plots show estimates for EURO-CORDEX data with the mean adjusted to ERA5-Land, and dark blue box plots show estimates for EURO-CORDEX data with the mean and standard deviation adjusted to ERA5-Land. The reference period for the adjustment is 1981-2010. Boxes (whiskers) indicate the interquartile range (minimum-to-maximum range) across EURO-CORDEX models.

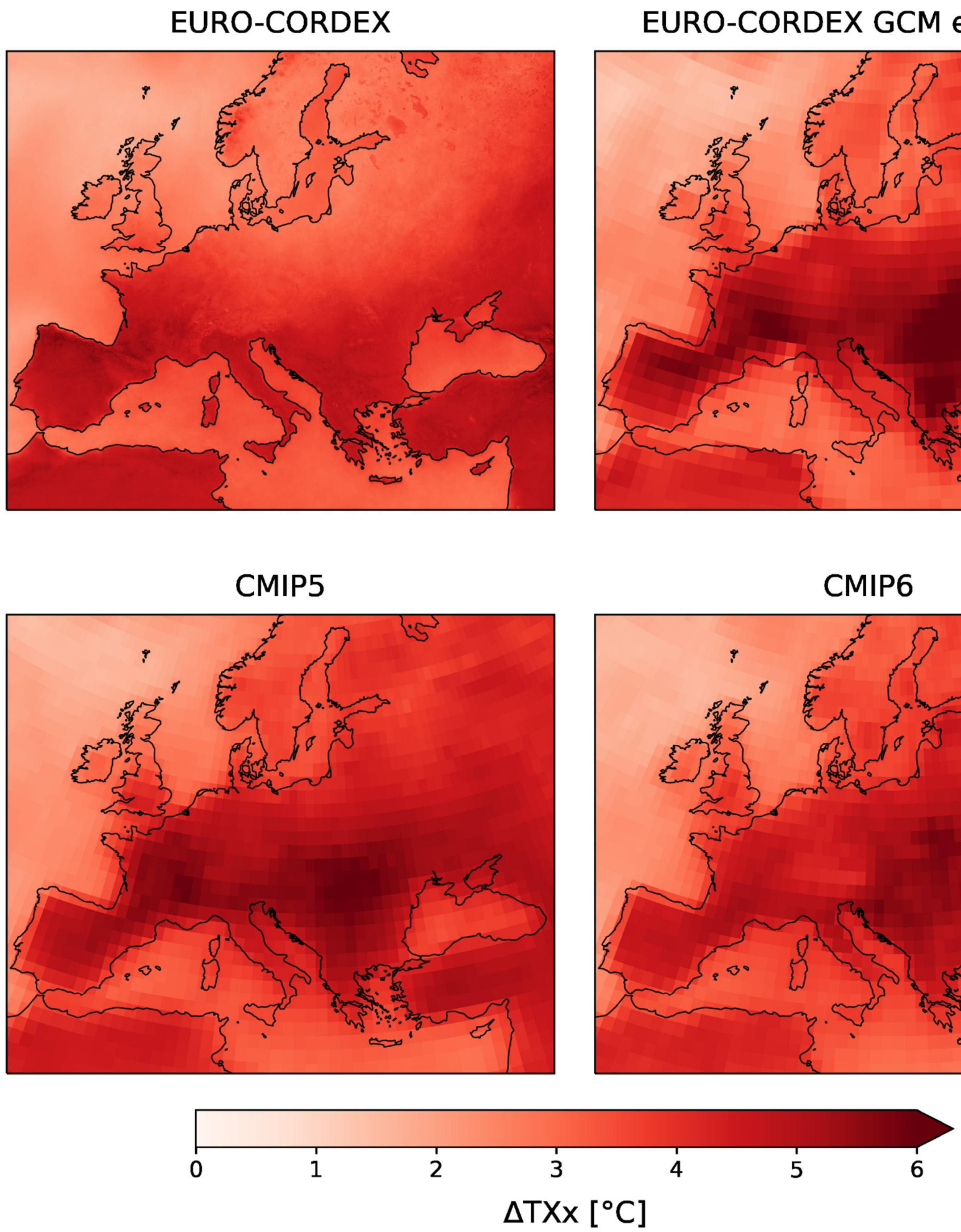

Figure S8: Multi-model median change in yearly maximum near-surface air temperature (ΔTXx) at 3 °C European warming relative to 1981-2010 for the EURO-CORDEX ensemble, the EURO-CORDEX GCM ensemble, the CMIP5 ensemble, and the CMIP6 ensemble according to the RCP8.5 scenario (EURO-CORDEX, EURO-CORDEX GCM ensemble, CMIP5) and the SSP5-8.5 scenario (CMIP6). Data for CMIP5 and CMIP6 were interpolated bilinearly to 1° resolution before calculating the multi-model median.